Nicotine Salt Pod System Temperature Regulation

Bill Alston
JUUL Labs, Inc., CA, USA

CORESTA SSPT CONFERENCE HAMBURG 2019
STPOST 03

Introduction

The JUUL system is a pre-filled (closed) nicotine salt pod system (NSPS) with automated temperature regulation mechanisms designed to minimize the generation of degradation products and to maintain consistency of temperature. There are no user-modifiable controls.

Purpose

The purpose of this study is to investigate the performance of the NSPS temperature control mechanism and to establish the accuracy of temperature control across a range of usage patterns and operating conditions through multiple means.

Methods

Actual atomizer transient wick-and-coil temperatures were measured simultaneously by infrared (IR) thermography, by electronic temperature control mechanisms within the device, and by sensors buried inside the fluid-conducting wick. Figures and plots are presented to illustrate transient temperature response. Techniques and results for pods having two different wick materials are described in detail.

IR temperature measurement requires an unobstructed view of the pod wick in the specific area where the heating coil (coil) is in contact. In order to provide such an unobstructed view, the pod was modified according to the following protocol. Modifications proceeded by removing the cover (**Fig. 1A**), bending back the electrical contact tabs (**Fig. 1B**), removing the wick and coil (**Fig. 1C**), cutting a rectangular window into the upstream side of the exposed polymer (**Fig. 1D**)[1], painting the viewable side of the coil with high temperature flat black paint (**Fig. 1E**), reassembling the pod and soldering the electrical contact tabs to stranded wire of specific gauge and length (**Fig. 1F**). A similar protocol was followed with the NSPS device such that device battery power and microprocessor temperature control algorithms can be applied during a simulated user experience (puff). Pod and device wires were connected with blade connectors for extremely low resistance.

Figure 1

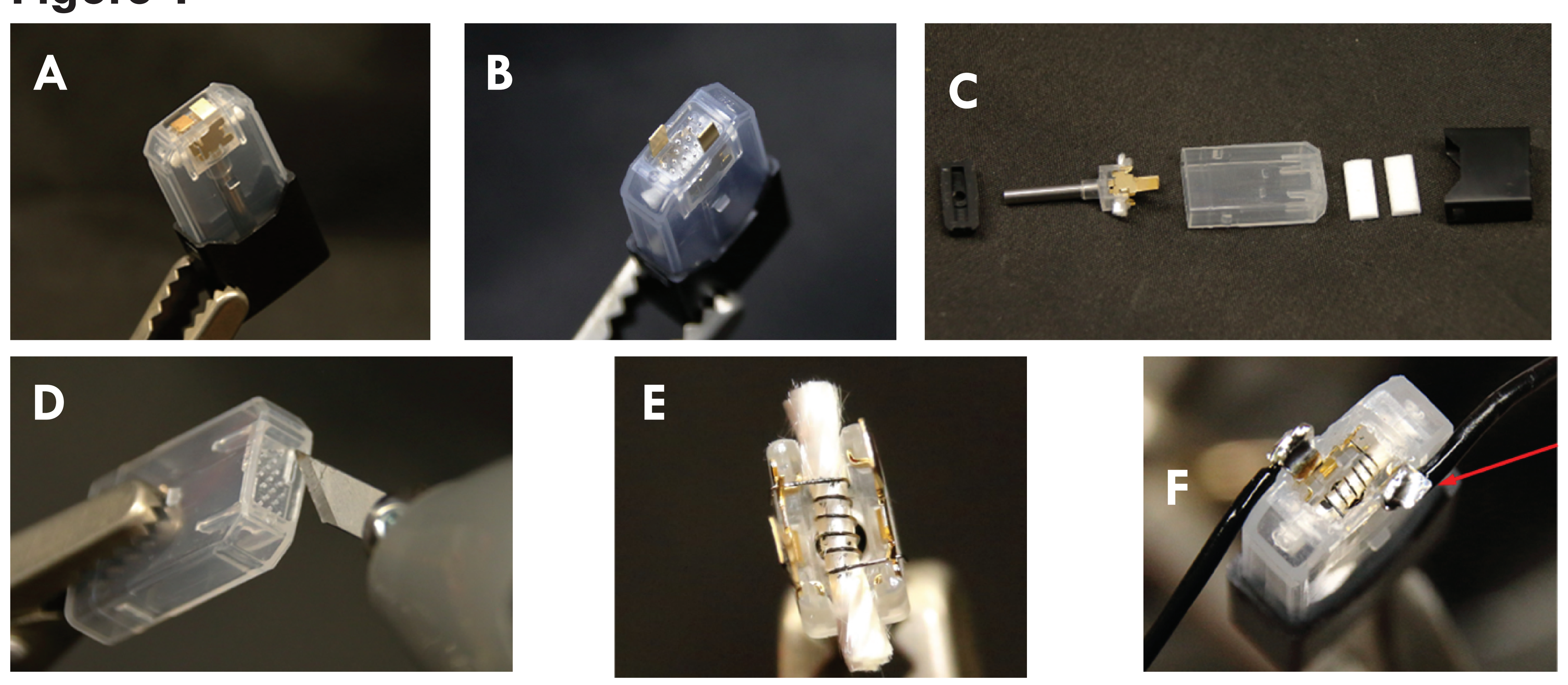

A typical puff is simulated by air flow control mechanism for fixed flow rate (1.4 liters per minute (LPM)), duration (3.0 seconds) and pause between puffs (30 seconds). Coil heating is activated by device internal microprocessor during the simulated puff. Both airflow and start sequence are controlled by computer for repetition of a typical ten puff sequence. Computer control also permits the capture and storage of information from the device microprocessor, to include temperature sensitive transient coil resistance and the resulting device response in applied power.

IR temperature measurements are performed with an Optris PI 450i IR camera fitted with a 90 mm focal length lens, as shown in **Fig. 2A**. The resulting images have a resolution of 388 x 288 pixels at a rate of 27 Hz, yielding continuous IR movies of the color-coded pod temperatures during puff sequences. A sample frame is shown in **Fig. 2B**. Captured within the pre-set Analysis Area is the wick and coil. Also shown in the frame is the instantaneous peak temperature within the Analysis Area that is captured in a separate file of peak surface temperatures vs. time. Note that painting the visible surface of the coil flat black (**Fig. 1E, F**) brings the combined saturated wick and coil to the approximate emissivity value of 0.96, as set in the IR camera controls.

[1] Therma-flow models show that opening the window in the upstream side of the pod has negligible effect on the wick and coil temperatures at typical user-produced flow rates.

Figure 2

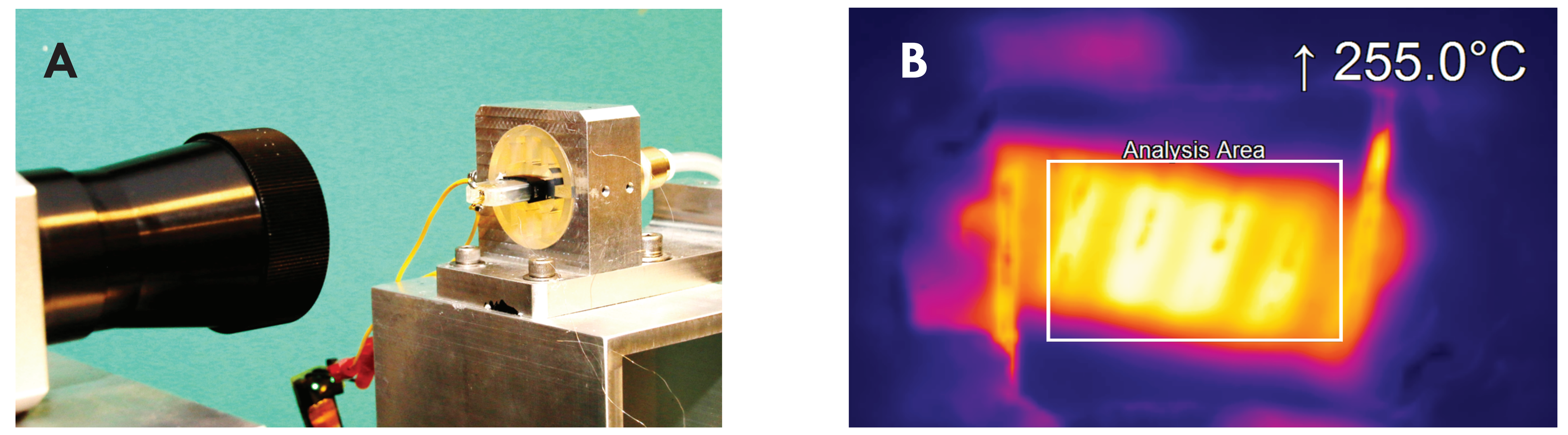

Thermocouples used are type K, 0.076 mm diameter, chosen to have extremely low thermal mass and therefore to have minimal effect on wick internal temperatures. Datalogger used is Dataq Model DI-245 with valid calibration from the National Institute of Standards and Technology (NIST).

Results

IR thermographic results yield both images and stored peak temperatures at each time step within the Analysis Area shown in **Fig. 2B**. These peak temperatures are plotted vs. time in a ten-puff sequence in **Fig. 3A** for glass fiber and in **Fig. 3B** for cotton wick. Ambient temperatures vary between 23°C and 25°C.

Figure 3

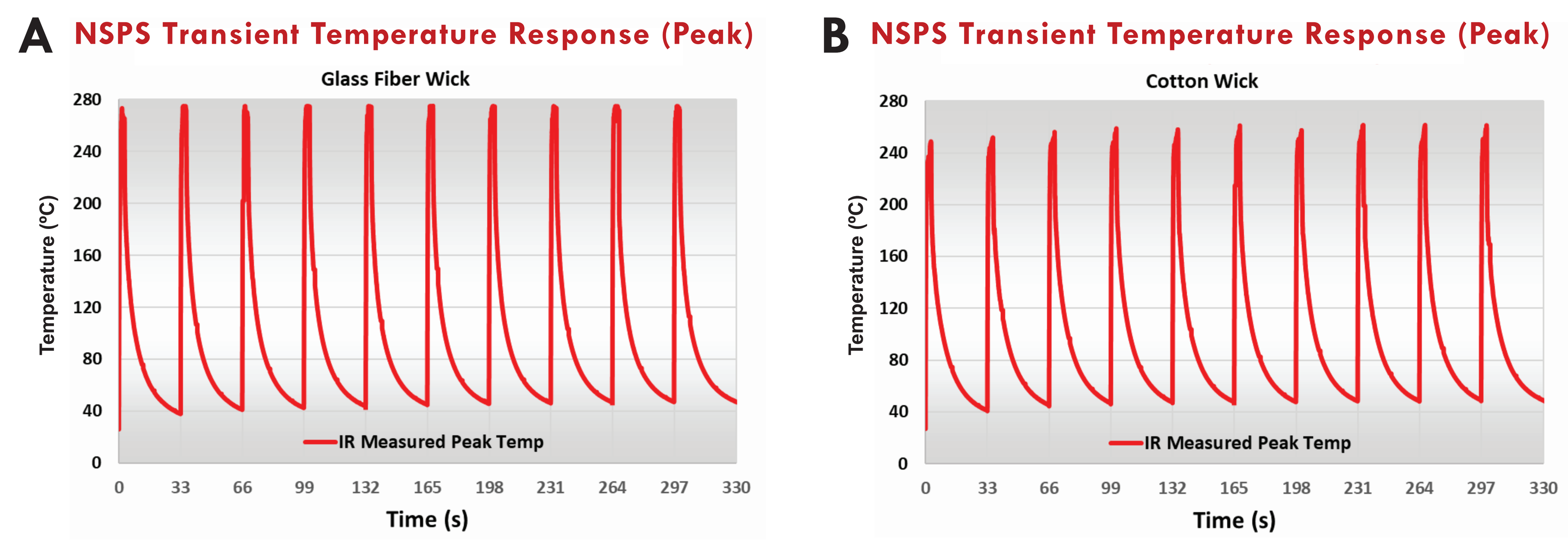

Simultaneously measured internal wick temperatures are plotted separately in **Fig. 4A** (glass fiber) and **FIG. 4B** (cotton), measured at wick center and plotted on the same thermal scale as above.

Figure 4

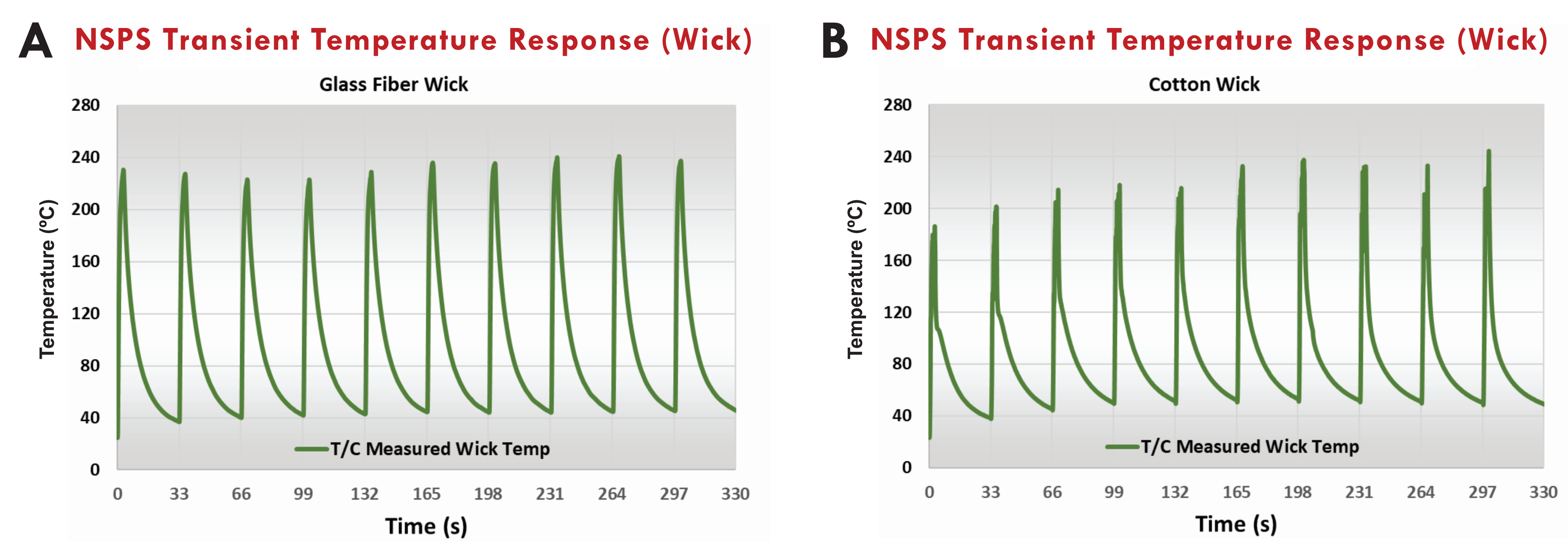

Notable are the temperature differences between glass fiber and cotton wicks, both at peak surface and internal wick values. Also notable is that peak temperatures never exceed 275°C even as internal wick fluid temperatures increase puff-to-puff. An explanation for these phenomena requires an introduction to the temperature control mechanisms to follow.

The NSPS coil temperature control is based on the coil metal temperature coefficient of resistivity (TCR), which results in a change of overall coil electrical resistance coincident with a change in coil temperature. Coil resistance is then an indicator of average coil temperature and is used as part of a microprocessor-driven algorithm to modulate coil power and to regulate temperature.

Shown in **Fig. 5A** is a plot of coil resistance in the ten-puff sequence of **Fig. 3A** and **Fig. 4A**, where the wick is glass fiber and coil resistance is recorded simultaneously. A similar plot is shown in **Fig. 5B**, where the wick is cotton in the ten-puff sequence of **Fig. 3B** and **FIG. 4B**. Plotted with live transient coil resistance in each case is the target coil resistance from which (through known TCR) is inferred the target coil temperature.

Figure 5

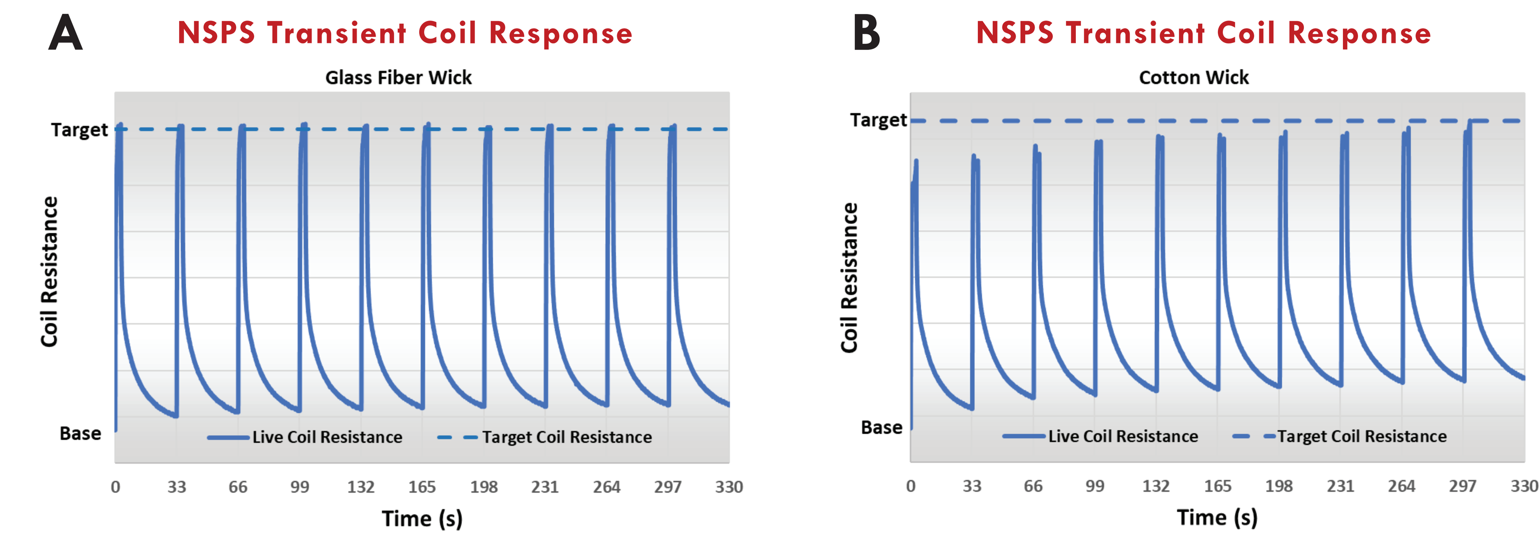

It can be seen in **Fig. 5A** with glass fiber wick the target resistance is achieved with each puff and manifests as peak temperatures of approximately 275 °C as shown in **Fig. 3B**. However, **Fig. 5B** shows that the cotton wick target resistance is not reached, which is reflected in the lower peak temperatures in **Fig. 3B**. It is probable that the lower temperatures with cotton wick are caused by the higher porosity relative to glass fiber and the resulting higher fluid saturation and higher vapor production. Higher fluid saturation results in higher thermal mass. The phase change with higher vapor production and coincident higher thermal load therefore limit peak temperature where the coil is in contact with the cotton wick, even as peak power is applied. Because coil power is modulated as a function of coil resistance, to indicate average coil temperature, coil leads not touching fluid can reach higher temperatures without consequence to fluid degradation.

Figure 6A shows averaged single-puff response of microprocessor control functions and resulting temperatures for glass fiber wick. Live coil and target resistances are plotted on the right vertical axis. Peak surface and internal wick temperatures are shown on the left vertical axis. Note that left and right vertical axes are arranged to avoid overlapping traces. **Figure 6B** shows a similar plot for cotton wick.

Figure 6

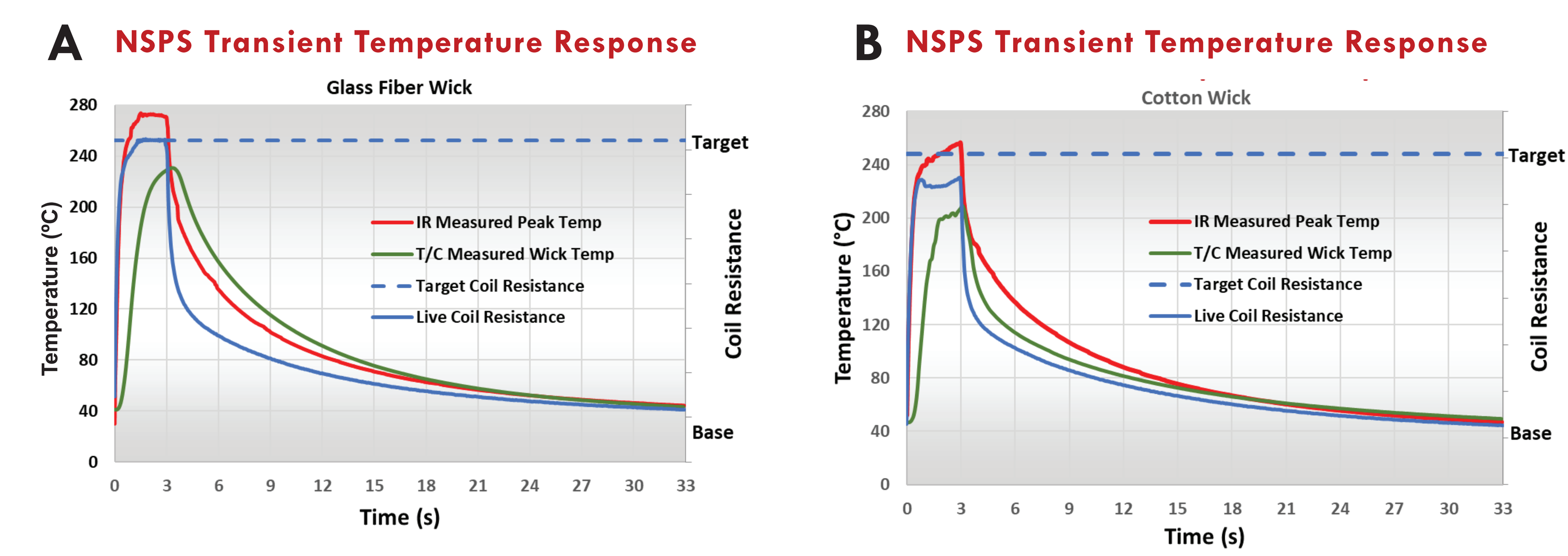

Conclusions

The NSPS method of microprocessor-driven temperature control utilizing coil metal TCR is successful in keeping maximum coil temperatures in contact with fluid saturated wick well below 300°C. This peak temperature control is shown for both glass fiber and cotton wicks having substantially different fluid delivery properties.

Higher thermal mass and higher vapor production, leading to higher thermal loads, result in lower temperatures in the cotton wick, both as surface peak values and more dramatically at wick center.